Evidence for a π junction in Nb/Ni_{0.96}V_{0.04}/Nb trilayers revealed by superfluid density measurements

M. J. Hinton, Stanley Steers, Bryan Peters, F. Y. Yang, and T. R. Lemberger

Phys. Rev. B **94**, 014518 — Published 29 July 2016

DOI: 10.1103/PhysRevB.94.014518

Evidence for a π-junction in Nb/$Ni_{0.96}V_{0.04}$/Nb Trilayers Revealed by Superfluid Density Measurements

M. J. Hinton, Stanley Steers, Bryan Peters, F.Y. Yang, T. R. Lemberger*

(Dated: July 15, 2016)

Abstract

We report measurements of the superfluid density, $\lambda^{-2}(T)$, in ferromagnet-on-superconductor (F/S) bilayers and S/F/S' trilayers comprising Nb with Ni, Py, CoFe, and NiV ferromagnets. Bilayers provide information about F/S interface transparency and the T dependence of λ^{-2} that inform interpretation of trilayer data. The Houzet-Meyer (H-M) theory accounts well for the measured dependence of $\lambda^{-2}(0)$ and T_c of F/S bilayers on thickness of F layer, d_F, except that $\lambda^{-2}(0)$ is slightly under expectations for CoFe/Nb bilayers. For Nb/F/Nb' trilayers, we are able to extract T_c and and λ^{-2} for both Nb layers when F is thick enough to weaken interlayer coupling. The lower "T_c" is actually a crossover identified by onset of superfluid in the lower-T_c Nb layer. For Nb/NiV/Nb' trilayers, $\lambda^{-2}(0)$ vs. d_F for both Nb layers has a minimum followed by a recovery, suggestive of a π-junction.

INTRODUCTION

Interest in the proximity effect between superconductors (S) and ferromagnets (F) has existed for some time, e.g., [1–7], and it continues as new measurements and ever more complex structures deepen understanding, e.g., [8–12]. Due to the spin-singlet state for the Cooper pairs of the BCS theory, ferromagnetism would be expected to realign the electron spins and destroy the Cooper pairing. Thus, when ferromagnetism and superconductivity coexist, such as when Cooper pairs propagate into an adjacent ferromagnet in the proximity effect, competition between the two states creates several new possibilities for superconductivity. These include the famed oscillation of the amplitude of the order parameter known as the Fulde-Ferrell-Larkin-Ovchinnikov state (FFLO)[8, 10, 13, 14], gapless superconductivity,[15] and π-junctions where the order parameter changes phase across the junction[2, 16, 17]. Such rich possibilities not otherwise found in superconductors or ferromagnets alone have led to both fundamental and practical interest in ferromagnetic/superconducting heterostructures, including as components of superconducting computational circuits [18].

There have been many measurements of T_c of F/S heterostructures as a function of the thickness d_F of the F layer, e.g., [1, 3–5, 8, 10, 11, 16, 17]. Many of them conclude that the effective exchange energy felt by Cooper pairs in the F layer is close to the Curie temperature, (i.e., $k_B T_C$), or higher. In theory of F/S structures, the exchange energy enters in the combination $2N_F(0)E_{ex}$, so determining E_{ex} requires a reliable value for $2N_F(0)$. We argued previously [11] that $2N_F(0)$ in $3d$ ferromagnets should be no smaller than the density of states in Nb, about 0.8×10^{29}/eV m^3,[19–21] and that would put the exchange energy about a factor of 3 smaller than $k_B T_C$. The present paper is an extension of our work on bilayers to trilayers.

The F/Nb bilayers discussed here include F = Ni, Py, CoFe, and the Nb/F/Nb' trilayers include F = Ni, NiV. The interesting thing about superfluid density measurements, as opposed to resistive measurements, is that they can provide transition temperatures and superfluid densities for both superconducting layers in S/F/S' trilayers. Surprisingly, we find that nominally identical Nb layers in S/F/S trilayers have different transition temperatures, presumably due to different S/F interface transparencies. This finding may have implications for analysis of resistive measurements of T_c on multilayer structures with multiple superconducting layers - T_c is that of the highest T_c S layer.

Two-coil measurements have been made for many years by many groups, e.g., [22–25]. In our version, we measure the mutual inductance between small coaxial coils on opposite sides of the

substrate that holds the sample. Typical measurement frequencies are 10 kHz to 50 kHz. The higher the sample's sheet conductivity, the more it attenuates the mutual inductance. A numerical analysis extracts the real and imaginary parts of the sheet conductivity of the sample, and from the latter we obtain areal superfluid density. For F/Nb bilayer samples, we present the data as volume superfluid density, $\lambda^{-2}(T)$, obtained by assuming that the superfluid is all in the Nb layer. For trilayers, the analysis is a little more involved, as explained below.

EXPERIMENTAL RESULTS AND DISCUSSION

Bilayers and trilayers are grown on 18 x 18 x 0.4 mm^3 oxidized silicon substrates by dc sputtering. Substrates are placed in a load-locked UHV system with a base pressure of $5x10^{-10}$ Torr. Ni, Nb, Py ($Ni_{0.8}Fe_{0.2}$), $Co_{0.5}Fe_{0.5}$, and $Ni_{0.95}V_{0.05}$ targets 2 inches in diameter, located 2 inches from the substrate, provide the material for deposition. In rapid succession, a layer of Ge (10.5 nm) is deposited, followed by Nb, F, and then for the trilayers, a top Nb layer that is usually thicker than the bottom Nb layer. All samples are protected with a 20 nm Ge layer on top. The Ge buffer layer on the oxidized silicon improves reproducibility. The deposition rates for Nb, Ge, CoFe, Py, and Ni are 1.5, 2.0, 1.30, 1.62, and 0.94 Å/s, respectively. Care was taken to avoid breaking vacuum between samples, and if vacuum was broken, samples were separated into different 'series' based upon when vacuum was broken. Cleanliness of this deposition chamber is better than before, so superfluid densities are as much as two times larger than found in an earlier study.[26]

As mentioned above, we use a two-coil technique to measure sheet conductivity, $d\sigma$, d = film thickness. When the sample is a single superconducting film, then conductivity, σ, is obtained by dividing $d\sigma$ by d. The penetration depth λ of the superconductor is related to σ_2 by: $\lambda^{-2} = \mu_0\omega\sigma_2$. In the literature, it is common to refer to $1/\lambda^2$ as the (volume) superfluid density. When the sample is a S/F bilayer, some superfluid may reside in the F layer. Nevertheless, we calculate volume superfluid density as if all of the superfluid were in the S layer, i.e., we divide sheet conductivity by the thickness of the S layer. For S/F/S' trilayers, analysis is a little more involved because superfluid resides in both superconducting layers.

F/S BILAYERS

There are several reasons to discuss bilayers in this paper on trilayers. First, we need them as a baseline for extracting effects due to inter-Nb-layer coupling: it is useful to compare the behavior of trilayers with that of two independent bilayers, the ultimate condition that obtains when the F layer is very thick. Second, data on bilayers establish that an appropriate function to use in fitting the T-dependence of superfluid density is dirty-limit BCS with a somewhat suppressed gap, as long as T_c has not been suppressed too much. Third, we want to show that superfluid density at $T = 0$ vs. suppressed T_c is in reasonable agreement with theory, despite the simplified nature of the theory.

Superfluid densities, $\lambda^{-2}(T)$, of several Py/Nb(250 Å) bilayers are shown in Fig. 1. As we find in all bilayer systems, T_c and $\lambda^{-2}(T)$ decrease together. Note the good sample-to-sample reproducibility, in the sense that small increases in d_{Py} produce correspondingly small decreases in T_c and $\lambda^{-2}(0)$. Transparency of the Nb/Py interface and exchange energy in Py are apparently quite reproducible. (We found that Ni/Nb bilayers are the least reproducible.) Magnetism in the Py layer is well-developed even at a thinness of 5 Å, as witnessed by the fact that T_c is already suppressed by 1.2 K. The maximum suppression of T_c is achieved at $d_F \approx 30$ Å, with data at $d_F = 100$ Å (not shown) being essentially identical with data at $d_F = 30$ Å.

CoFe/Nb(250 Å) bilayers, Fig. 2, behave similarly to Py/Nb(250 Å) bilayers, Fig. 1, except that the maximum suppression of T_c is 50% larger. Given that the Nb layers have the same thickness, theory accounts for this difference in terms of a difference in interface transparency; CoFe/Nb interfaces are more transparent to electrons than Py/Nb interfaces. Note that the bilayer with the thickest CoFe layer, 100 Å, has a T_c a bit higher than the bilayer with $d_{CoFe} = 40$ Å, suggesting that T_c may have a shallow minimum.

We emphasize that for bilayers with $T_c \approx 6$ K and above, $\lambda^{-2}(T)$ at low-T is BCS like, i.e., flatter than quadratic, but with a gap somewhat smaller than for pure Nb films. For bilayers with more strongly suppressed T_c's, $T_c \approx 4$ K and below, the low-T behavior is more quadratic. These behaviors are important when analyzing trilayers.

We consider these results in the context of dirty-limit theory [27] based on a previous paper. In our earlier analysis of T_c vs. d_F for various bilayers involving 3d ferromagnets, [11] both our own data and data from the literature, we found that the clean-limit Cooper pair coherence length in F, $\xi_{F0} = \hbar v_{F,F}/E_{ex}$, is typically about 10 nm while the electron elastic mean-free-path in F, ℓ_F, is only

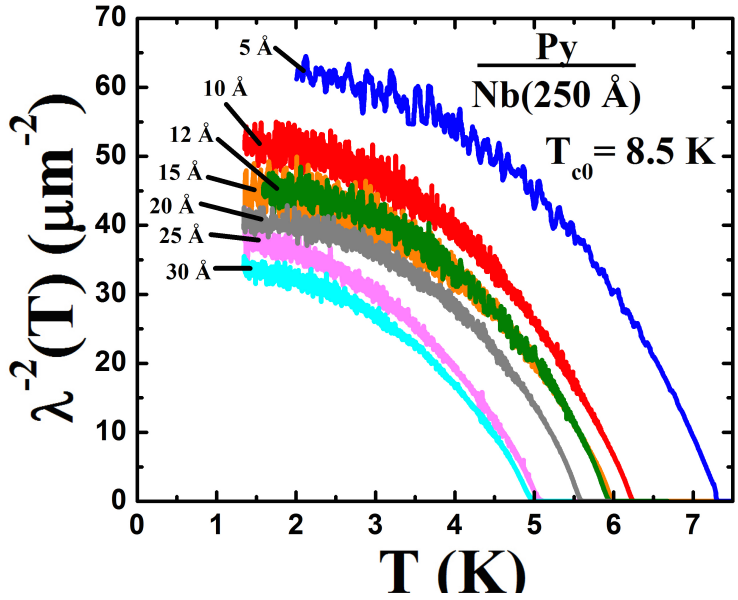

FIG. 1. $\lambda^{-2}(T)$ of Py/Nb(250 Å) bilayers with d_{Py} = 5 - 30 Å. T_{c0} = 8.5 K for d_{Nb} = 250 Å (not shown). Also not shown, Py(100 Å), which has identical $\lambda^{-2}(T)$ to d_{Py} = 30 Å.

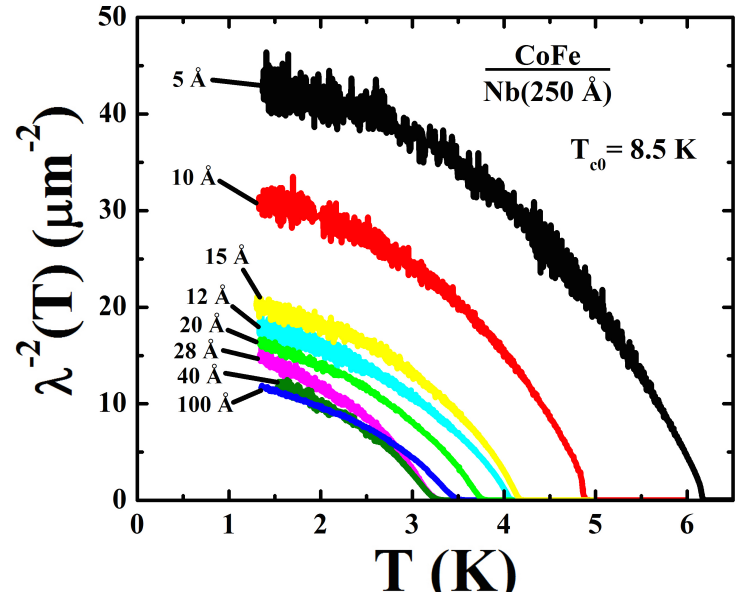

FIG. 2. $\lambda^{-2}(T)$ of CoFe/Nb bilayers with d_{Nb} = 250 Å and d_{CoFe} = 5 to 100 Å. T_{c0} = 8.5 K for d_{Nb} = 250 Å.

a few nm. These values are based on two reasonable assumptions. First, that the effective electron density of states in 3d ferromagnets is no smaller than the density of states in Nb, or, equivalently,

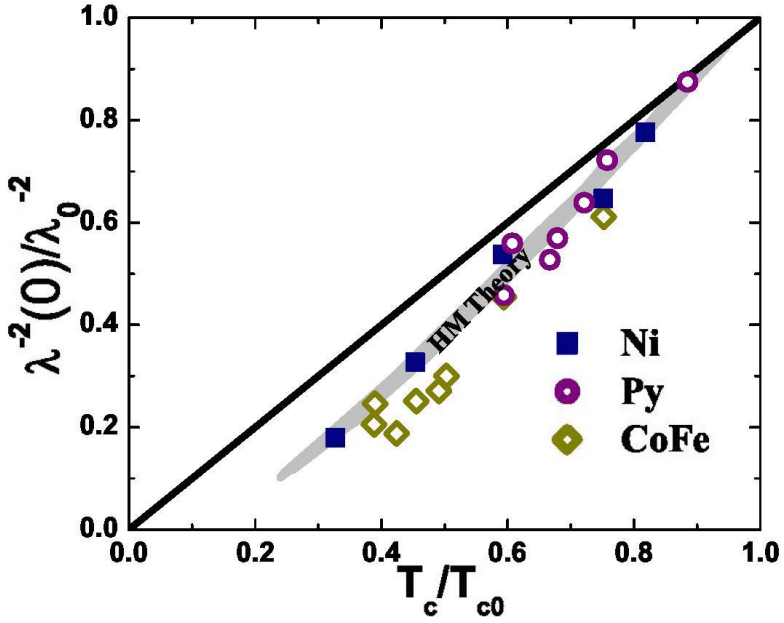

FIG. 3. $\lambda^{-2}(0)/\lambda_0^{-2}(0)$ vs. T_c/T_{c0} for Ni/Nb, Py/Nb and CoFe/Nb bilayers. $\lambda_0^{-2}(0)$ is the superfluid density of a plain Nb film of the relevant thickness. H-M theory is represented by the grey arc. The black line represents $\lambda^{-2}(0) \propto T_c$. The Ni/Nb and Py/Nb data fall on the theory. For CoFe/Nb, $\lambda^{-2}(0)/\lambda_0^{-2}(0)$ is lower than expected.

that the electron diffusion constant in F is about equal to the diffusion constant in Nb, ≈ 3 cm$^2/s$, derived from measurements of the upper critical field in Nb films about 10 nm thick. Second, that the Fermi velocity in F, $v_{F,F}$, is about 5×10^5 m/s, a typical value. Thus, dirty-limit theory is appropriate.

Clean-limit and dirty limit theory[4, 27, 28] agree on T_c vs. d_F when the F layer is thinner than an electron mean-free-path, $d_F << \ell_F$. Both find that, in effect, in this regime Cooper pairs in F bounce ballistically back and forth through the F layer, hitting the F/S interface on each pass, and occasionally passing back through the F/S interface. Dirty-limit theory differs from clean-limit theory mainly because when $d_F > \ell_F$ significant numbers of Cooper pairs in F return to the F/S interface by bouncing off of impurities rather than having to go all the way to the back of the F layer. Our previous paper concluded that interface transparencies are such that a typical electron in F hits the F/S interface about three times before getting through.

Figure 3 compares normalized superfluid densities at $T = 0$ with Houzet-Meyer (H-M) theory[27]. It shows $\lambda^{-2}(0)$ and T_c from Figs. 1, and 2, plus data on Ni/Nb bilayers not shown here. The black

line represents the linear-in-T_c reduction in $\lambda^{-2}(0)$ that would occur if the suppression of T_c were due solely to a reduction in the pairing interaction, assuming dirty-limit BCS applies. The grey area marked "Theory" represents the allowed values given by Houzet-Meyer theory throughout all of parameter space. The Ni/Nb and Py/Nb data clearly agree with the theory. The CoFe/Nb data fall consistently below expectations, especially for $T_c/T_{c0} \leq 0.6$. We do not understand why this particular bilayer system should disagree with theory while the others agree. Perhaps it has something to do with the thickness of the Nb layer being somewhat larger than the BCS coherence length. In that case, it might have shown up in the Py/Nb bilayers if they had had lower T_c's. Perhaps it is related to the higher exchange energy in CoFe.

With the basic qualitative and quantitative understanding of superfluid density in S/F bilayers established in this section, we are prepared to study trilayers.

Nb/Ni/Nb' AND Nb/NiV/Nb' TRILAYERS

Nb/Ni/Nb'

The exciting thing about superfluid density measurements is that T_c and superfluid densities of the two superconducting layers can be determined separately. This complements other probes. For example, resistive determinations of T_c of multilayers tell us only the T_c of the layer with the highest T_c; tunneling measurements observe the layer being tunneled into.

We begin with superfluid densities, $\lambda^{-2}(T)$, for trilayers of Nb(d_{Nb})/Ni(150 Å)/Nb(125 Å), with the top Nb layer having various thicknesses, $d_{Nb} = 105$, 125, and 150 Å, Fig. 4. The Ni layer is thick so that these trilayers are effectively two independent bilayers with different T_c's and superfluid densities. Fits to data in the figure are explained below. Volume superfluid density in the figure is arbitrarily obtained by dividing the measured areal superfluid density by 125 Å, the thickness of the bottom Nb layer. Analysis consists of determining the superfluid densities and T_c's of the two Nb layers.

It is clear in Fig. 4 that there are upper T_c's (at about 4 K, 5 K, and 6 K) that increase with the thickness of the upper Nb layer, so these are the T_c's of the upper "bilayers". And there is a kink at about 3.3 K that must be T_c of the lower Nb layer since this layer has the same thickness in all three samples. Strictly speaking, this is a crossover temperature because there is some coupling through the Ni film, thick though it be, so that there are Cooper pairs in the lower Nb layer as soon

as the top layer goes superconducting, but we refer to it as a transition for simplicity.

Why does the upper Nb layer have a higher T_c even when it is thinner than the lower layer and is in contact with the same Ni layer? Possibly the upper Nb layer has a higher intrinsic T_c because it grows on Ni whereas the lower layer grows on amorphous Ge. We think it more likely that the lower S/F interface has a higher transparency (or, lower specific resistance) than the upper interface. This is the only explanation allowed by theory, if magnetism is uniform through the thickness of the Ni layer. There are suggestions in the literature that magnetism varies in Ni films, e.g., there may be a magnetically "dead" layer at the bottom of the film, or an increase in Curie temperature from bottom to top. In either case, magnetism would be stronger on the top of the Ni layer, so one might expect Ni to have a stronger effect on T_c of the upper Nb layer, opposite to what happens. We conclude that the lower Nb layer is in better contact with the Ni layer. Our analysis finds that, in classical terms, a typical electron in Ni has to hit the upper Ni/Nb interface about 4 times to get through, but only about 2.5 times for the lower interface.

From the foregoing discussion, it is clear that superfluid at $T > 3.3$ K resides in the upper Nb layers, so it is easy to get $\lambda^{-2}(T)$ above 3.3 K by dividing the measured areal superfluid density by the upper-layer thickness. We get $\lambda^{-2}(0)$ and T_c, Table I, by fitting $\lambda^{-2}(T)$ with an appropriate function. For samples with T_c's of 5 K and 6 K, we get good fits with the usual dirty-limit BCS form, with a suppressed gap, $\Delta(0)/k_B T_c \approx 1.6$. (Our conclusions are insensitive to the exact gap value.) For the sample with $T_c = 4$ K, we fit data from 3.4 K to 4 K with a two-term quadratic. Clearly there is some ambiguity in exactly what function to use, and that plays into error bars on $\lambda^{-2}(0)$ for the lower layer. For all samples, we fit data below 3 K with a two-term quadratic. We obtain the superfluid density of the lower Nb layer by subtracting that of the upper Nb layer from the total. We find: $\lambda^{-2}(0) \approx 18$, 26, and 38 μm^{-2}, or, 28 ± 10 μm^{-2} for the lower Nb layer. Given $T_c/T_{c0} \approx 3.3/8$ and $\lambda^{-2}(0) \approx 90$ μm^{-2} for a Nb(125 Å) film (measured separately), then theory in Fig. 4 predicts that the lower Nb layer should have: $\lambda^{-2}(0) \approx 25$ μm^{-2}, so our experimental values are reasonable. The upshot is that it is possible to obtain the superfluid density of both layers, but there is significant uncertainty in $\lambda^{-2}(0)$ for the lower layer.

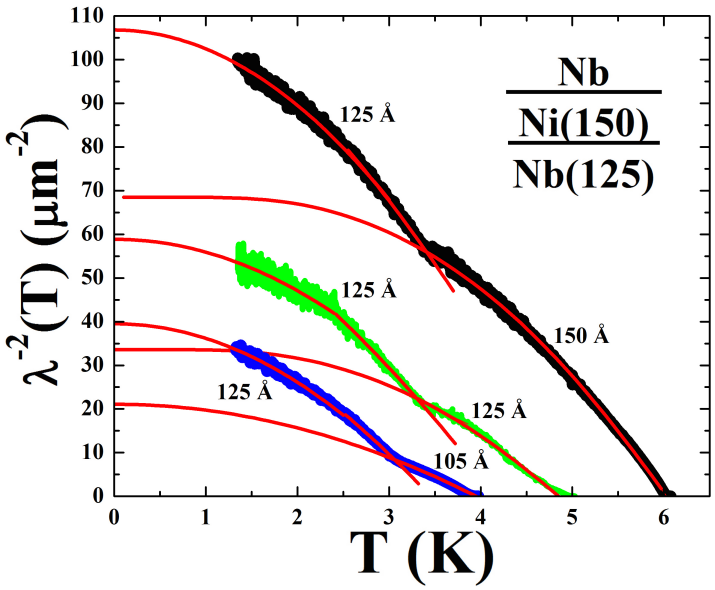

FIG. 4. Here $\lambda^{-2}(T)$ is areal superfluid density of Nb/Ni(150 Å)/Nb(125 Å) trilayers divided by the 125 Å thickness of the bottom Nb layer. The top Nb layers have thicknesses of 105, 125, and 150 Å. The Ni layer is thick so that coupling between Nb layers is minimal, and there are two distinct transitions, the lower one at about 3.3 K in all trilayers. Fits to $\lambda^{-2}(T)$ at $T < 3.3$ K are two-term quadratics. Fits to $\lambda^{-2}(T)$ at $T > 3.4$ K for the trilayers with upper T_c's of 5 K and 6 K are of the dirty-limit BCS form with reduced gaps. See text. The intersection of fits defines the effective T_c of the lower Ni/Nb bilayer.

TABLE I. Values of $\lambda^{-2}(0)$ and T_c for top and bottom Nb layers, and the gap energy $\Delta(0)/k_BT_c$ used for BCS fits to $\lambda^{-2}(T)$ of the upper layers with $d_{Nb} = 125$ Å and 150 Å. For $d_{Nb} = 125$ Å a two-term quadratic fit was used.

d_{Nb} (top)	$\lambda^{-2}(0)$ (top)	$\lambda^{-2}(0)$ (bottom)	T_c (top)	T_c (bottom)	$\Delta(0)/k_BT_c$
Å	μm^{-2}	μm^{-2}	K	K	
150	57	38	6.02	3.42	1.61
125	34	25	4.85	3.30	1.62
105	25	18	3.95	3.06	quad.

Nb/NiV/Nb'

In growing the trilayers discussed in this section, we took care to minimize the time between depositions of layers in order to minimize interface resistances. Our focus is on coupling of Nb layers through the ferromagnetic NiV layer, so we study superfluid density vs d_{NiV}. We chose to use a ferromagnet with a smaller Curie temperature than Ni - $T_C = 400$ K for $Ni_{0.96}V_{0.04}$.

[29] Figure 5 shows areal superfluid densities of many Nb(200 Å)-on-$Ni_{0.96}V_{0.04}$-on-Nb(125 Å) trilayers. [Trilayers with NiV thicknesses of 30 Å and 45 Å fit right in where they should, but they are not shown for clarity.] The temperature where superfluid first appears is naturally identified as T_c of the upper, thicker, Nb layer. The maximum suppression of this T_c is about 2.7 K. At first, $\lambda^{-2}(0)$ decreases as d_{NiV} increases, but then it increases while T_c remains constant at about 5.7 K. This is suggestive of a transition to a π-junction at $d_{NiV} \approx 30$ Å, as discussed below.

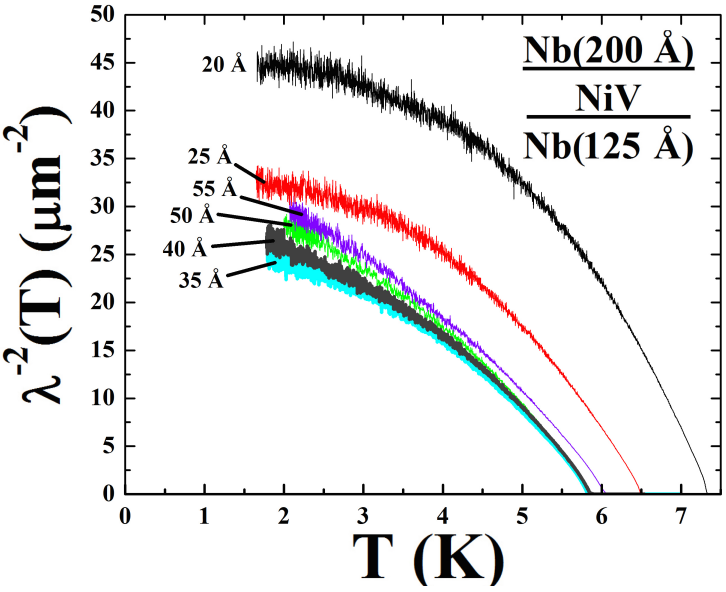

FIG. 5. Superfluid densities of Nb(200 Å)/NiV/Nb(125 Å) trilayers normalized to the total Nb thickness, 325 Å. NiV thickness ranges from 20 Å to 55 Å. $\lambda^{-2}(0)$ and T_c decrease as NiV thickness increases to 30 Å, after which $\lambda^{-2}(0)$ increases while T_c is nearly constant.

To highlight the effect of coupling between Nb layers, Fig. 6 compares $\lambda^{-2}(T)$ of trilayers with the thinnest (20 Å) and thickest (55 Å) NiV layers. The former has a T_c only 1 K below that of a plain 200 Å Nb film, and dirty-limit BCS describes $\lambda^{-2}(T)$ with an unsuppressed gap, $\Delta(0)/k_B T_c = 1.9$, the same value found for Nb films.[26] This trilayer behaves like a single film because coupling between Nb layers is large and pair-breaking from the NiV layer is small. The same is true for the NiV(25 Å) trilayer. For these two trilayers we cannot determine $\lambda^{-2}(0)$ for each Nb layer, only its average value.

We see in Fig. 6 that $\lambda^{-2}(T)$ for the 55 Å NiV trilayer shows much less downward curvature than the 20 Å NiV trilayer. T_c of the 55 Å NiV trilayer is lower due to increased pair-breaking. It is not obvious from the data that the explanation is a second transition (a crossover, to be precise)

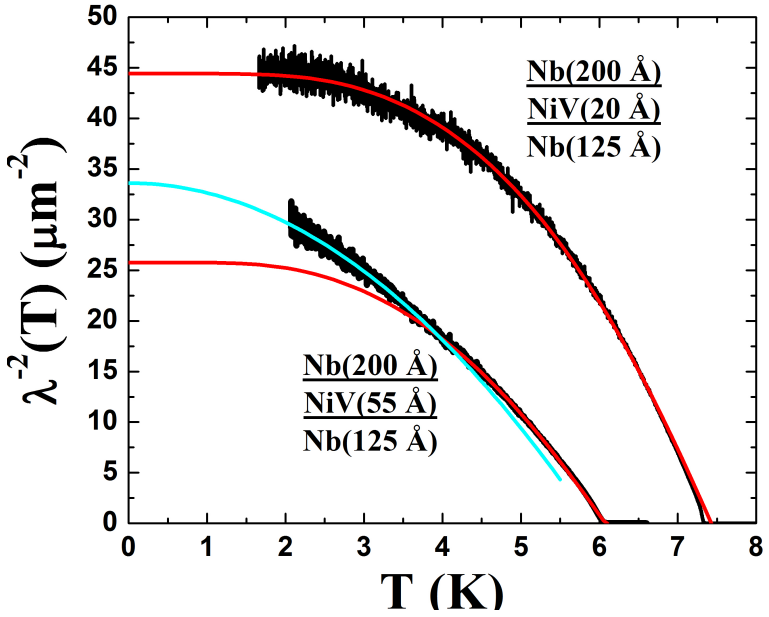

FIG. 6. $\lambda^{-2}(T)$ of Nb(200 Å)/NiV/Nb(125 Å) trilayers with the thinnest (upper data) and thickest (lower data) NiV layers. The former is well described by dirty-limit BCS with a full gap, $\Delta(0)/k_BT_c = 1.9$ (red curve). The latter is well described by dirty-limit BCS with a slightly suppressed gap, $\Delta(0)/k_BT_c = 1.7$, only for T>4 K (red curve). The low-T data are fitted by a quadratic, $\lambda^{-2}(T)/\lambda^{-2}(0) = 1 - AT^2$. T_c of the lower Nb layer is defined at the intersection of fits.

at about 3.5 K, but we would certainly expect a second transition for trilayers with a very thick F layer, as we saw for Nb/Ni/Nb' trilayers in the previous section. Thus, we analyze $\lambda^{-2}(T)$ as if the trilayer were two independent bilayers. In Fig. 6 we find a good fit of $\lambda^{-2}(T > 4K)$ to dirty-limit BCS with a suppressed gap $\Delta(0)/k_BT_c \approx 1.7$, but there is "excess" superfluid at T<3.5 K that we assign to the lower Nb layer. The rest of the analysis for trilayers with $d_{NiV} \geq 30$ Å is the same as for Nb/Ni/Nb layers in the previous section. Until there appears a theory for superfluid density in S/F/S' trilayers, this is the most reasonable way to proceed.

As a quick check on the reasonableness of the analysis so far, we compare T_c vs. d_{NiV} for both Nb layers, Fig. 7, with theory. The figure shows T_c vs. d_{NiV} for the upper Nb(200 Å) layer (upper data) and lower Nb(125 Å) layer (lower data). Theoretical fits to Houzet-Meyer theory (gray curves) were done as if the trilayer were two independent bilayers, as done in ref. [11]. Resulting fit parameters are: dirty-limit cooper-pair coherence length in NiV, $\xi_F = 35$ Å, which is about the same as was found for F/Nb bilayers with F = Ni, Py, and CoFe,[11], and exchange energy $E_{ex} = 4.2$ meV (≈ 50 K), assuming that the effective electron density of states in NiV is the same as the density of states in Nb. This is about 8 times smaller than $k_BT_C \approx 35$ meV for NiV. Since

the Nb films probe the same NiV film, ξ_F and E_{ex} should be the same for both fits and they are. Just as we found in Nb/Ni/Nb trilayers, the upper Nb/NiV interface resistance, $R_b = 2.1 f\Omega\cdot\mathrm{m}^2$, is slightly larger than for the lower interface, $R_b = 1.75 f\Omega\cdot\mathrm{m}^2$. Quantitatively, these resistances are in line with values for other Nb/F bilayers.[11]

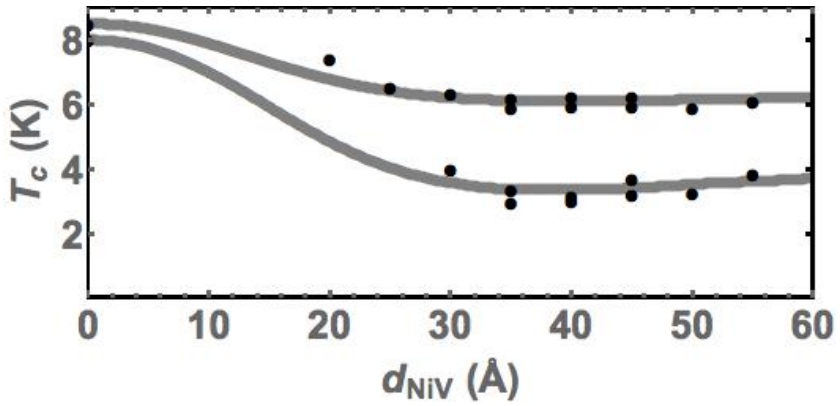

FIG. 7. T_c vs. d_{NiV} for Nb(200 Å) layers (upper data points) and Nb(125 Å) layers (lower data points) of Nb/NiV/Nb trilayers. Theoretical fits to Houzet-Meyer theory for bilayers were done as described in ref. [11]. Fit parameters are discussed in the text.

The main result of this paper is in Fig. 8, which shows $\lambda^{-2}(0)$ vs. d_{NiV} for both Nb layers in Nb/NiV/Nb' trilayers. We made two sets of samples. Data for each set are connected by solid or dashed curves. "Theory" curves in the figure are generated from the theory curve in Fig. 3 and the measured T_c/T_{c0}'s, with $T_{c0} = 8$ K and 8.5 K for $d_{Nb} = 125$ Å and 200 Å, respectively. Fitted values of $\lambda^{-2}(0)$ for plain Nb(200 Å) and Nb(125 Å) "monolayers", i.e., values of $\lambda^{-2}(0)$ at $d_{NiV} = 0$, are chosen so that theory fits data at $d_{NiV} = 55$ Å. They are consistent with measurements on plain Nb films.

For $d_{NiV} \geq 30$ Å, $\lambda^{-2}(0)$ increases for both Nb layers, the more so for the thinner one. For $d_{NiV} = 20$ Å and 25 Å, the Nb layers are strongly coupled, and their superfluid responses turn on together. Our analysis methodology assigns all of the superfluid to the upper Nb layer for these trilayers, so in the figure it looks like $\lambda^{-2}(0)$ of the upper Nb layer is surprisingly large while $\lambda^{-2}(0)$ for the lower Nb layer is zero. However, the measured areal superfluid density is also consistent with each Nb layer having the volume superfluid density indicated by the open circles at $d_{NiV} = 20$ Å and 25 Å. At $d_{NiV} = 20$ Å, this division of superfluid looks reasonable. However, at $d_{NiV} = 25$ Å, there is a shortage of superfluid. We take this as evidence for a transition to a π-junction. For reference, we note that Kushnir et al. [17] see the transition to a π-junction in

Nb/$Cu_{0.41}Ni_{0.59}$/Nb trilayers at $d_{CuNi} \approx 5$ nm. Given that the Curie temperature of our NiV is about twice that of $Cu_{0.41}Ni_{0.59}$, our transition at $d_{NiV} \approx 3$ nm looks reasonable.

We recognize that the overall agreement of theory with experiment looks pretty good, but the slow rise in $\lambda^{-2}(0)$'s with increasing d_{NiV} is puzzling. For the thicker Nb layer, the increase is not accounted for by the change in T_c with d_{NiV} because T_c actually decreases slightly. And the rise cannot be a transfer of superfluid from lower to upper Nb layer because both increase. We propose the following rough picture, illustrated in Fig. 9, which shows the superconducting order parameter $\Psi(x)$ through the thickness of the trilayer. The local superfluid density is proportional to $|\Psi|^2$. For $d_{NiV} < 30$ Å, $\Psi(x)$ has a minimum inside the NiV layer. Ψ in the Nb layers is only weakly suppressed at the Nb/NiV interfaces. Then, around $d_{NiV} = 30$ Å, coupling between Nb layers changes to a π junction, with the order parameter changing sign inside the NiV. Now $\Psi(x)$ is strongly suppressed in the Nb layers where they contact the NiV, coupling between Nb layers weakens dramatically, and the lower transition becomes apparent in $\lambda^{-2}(T)$. As d_{NiV} increases further, Ψ at both interfaces increases, so $\lambda^{-2}(0)$ increases in both layers.

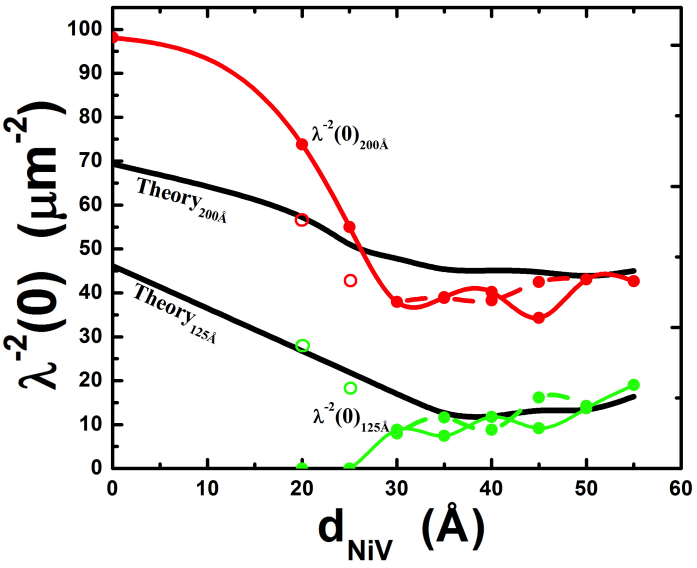

FIG. 8. Superfluid densities $\lambda^{-2}(0)$ attributed to the 200 Å and 125 Å Nb layers in Nb(200 Å)-on-NiV-on-Nb(125 Å) trilayers. The dashed and solid lines connect data taken from different growth series. Theory curves and open circle data points are described in the text.

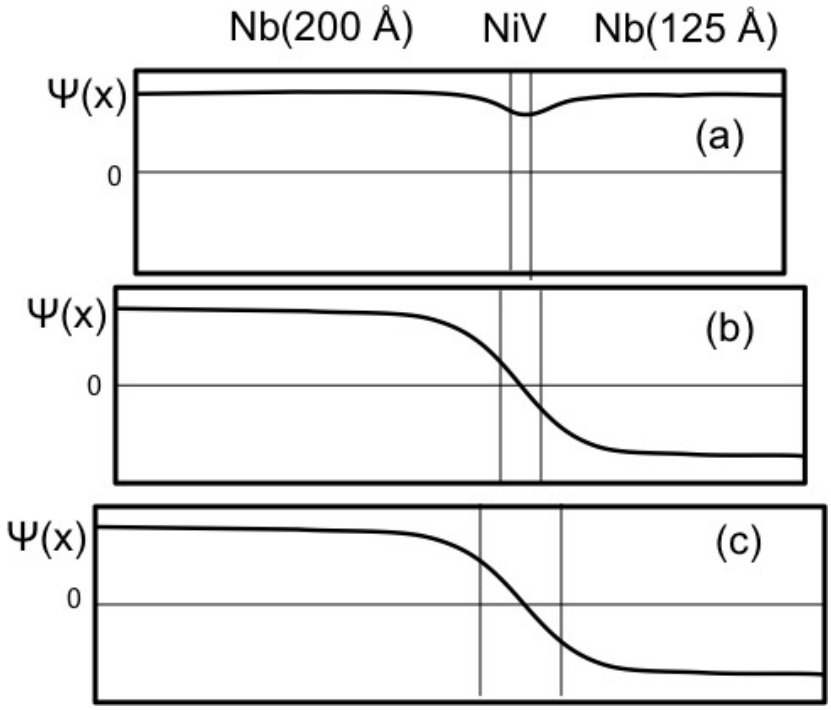

FIG. 9. (a) There is a shallow dip in $\Psi(x)$ inside the NiV layer when the NiV layer is thin. (b) $\Psi(x)$ changes sign inside the NiV layer when the layer is thicker, forming a π-junction that substantially reduces Ψ in the Nb layers at the Nb/NiV interfaces, thereby reducing $\lambda^{-2} \propto |\Psi|^2$. (c) As d_{NiV} increases further, the suppression of Ψ relaxes so $\lambda^{-2}(0)$ increases.

CONCLUSION

Superfluid densities of sputtered F-on-S bilayers - Py/Nb, CoFe/Nb, and Ni/Nb - with various thicknesses of F layers show that $\lambda^{-2}(T)$ loses its BCS-like flatness at low T when T_c is strongly suppressed, as expected when superconductivity is suppressed by Cooper pair-breaking. $\lambda^{-2}(0)/\lambda_0^{-2}(0)$ vs. T_c/T_{c0} for bilayers is in generally good agreement with theory, except that superfluid densities for CoFe/Nb bilayers are a little lower than theory predicts.

Superfluid densities of Nb/Ni/Nb' trilayers with very thick Ni layers clearly show that each Nb layer has its own superconducting transition and that one can determine T_c and superfluid densities for both Nb layers when coupling between them is weak. The fact that nominally identical Nb films in contact with opposite sides of the same thick Ni film can have different T_c's strongly suggests that F/S interface transparency is the dominant factor in determining the maximum suppression of T_c, not the exchange energy in F.

Superfluid densities of Nb/NiV/Nb trilayers provide insight into the evolution of superconduc-

tivity from strong to weak interlayer coupling. For NiV less than 30 Å thick, Nb layers are strongly coupled and superfluid in the lower Nb layer turns on at the T_c of the upper layer. At $d_{NiV} \approx 30$ Å there is a qualitative change - a significant amount of superfluid turns on at a lower T_c and less at the upper T_c. This qualitative change suggests a transition to π-junction coupling between Nb layers. This interpretation accounts qualitatively for the gradual increase in superfluid density in both Nb layers as d_{NiV} increases from 30 to 55 Å.

This work was supported in part by NSF grant DMR-0805227. We acknowledge useful discussions with Jan Aarts, Christoph Strunk, and Norman Birge.

* trl@physics.osu.edu

[1] J. Aarts, J. M. E. Geers, E. Brück, A. A. Golubov, and R. Coehoorn, Physical Review B **56**, 2779 (1997).

[2] V. V. Ryazanov, V. A. Oboznov, A. Y. Rusanov, A. V. Veretennikov, A. A. Golubov, and J. Aarts, Physical Review Letters **86**, 2427 (2001).

[3] Y. V. Fominov, N. M. Chtchelkatchev, and A. A. Golubov, Physical Review B **66**, 014507 (2002).

[4] A. Sidorenko, V. Zdravkov, A. Prepelitsa, C. Helbig, Y. Luo, S. Gsell, M. Schreck, S. Klimm, S. Horn, L. Tagirov, and R. Tidecks, Annalen der Physik **12**, 37 (2003).

[5] J. Kim, J. H. Kwon, K. Char, H. Doh, and H.-Y. Choi, Physical Review B **72**, 014518 (2005).

[6] A. Buzdin, Reviews of Modern Physics **77**, 935 (2005).

[7] F. S. Bergeret, A. F. Volkov, and K. B. Efetov, Reviews of Modern Physics **77**, 1321 (2005).

[8] V. I. Zdravkov, J. Kehrle, G. Obermeier, A. Ullrich, S. Gsell, D. Lenk, C. Müller, R. Morari, A. S. Sidorenko, V. V. Ryazanov, L. R. Tagirov, R. Tidecks, and S. Horn, Superconductor Science and Technology **24**, 095004 (2011).

[9] K. M. Boden, W. P. Pratt, and N. O. Birge, Physical Review B **84**, 020510 (2011).

[10] J. Kehrle, V. I. Zdravkov, G. Obermeier, J. Garcia-Garcia, A. Ullrich, C. Mueller, R. Morari, A. S. Sidorenko, S. Horn, L. R. Tagirov, and R. Tidecks, Annalen der Physik **v524**, 37 (2012).

[11] T. R. Lemberger, M. J. Hinton, J. Yong, J. M. Lucy, A. J. Hauser, and F. Y. Yang, Journal of Superconductivity and Novel Magnetism (2014).

[12] M. Eschrig, Physics Today **64**, 43 (2011).

[13] P. Fulde and R. A. Ferrell, Physical Review **135**, A550 (1964).

[14] A. I. Larkin and Y. N. Ovchinnikov, Soviet Physics-JETP **20**, 762 (1965).

[15] K. Maki, *Superconductivity*, edited by R. Parks (Marcel-Dekker, New York, New York, 1969) pp. 1051–1053.

[16] V. N. Kushnir, S. L. Prischepa, C. Cirillo, A. Vecchione, C. Attanasio, M. Y. Kupriyanov, and J. Aarts, Physical Review B **84**, 214512 (2011).

[17] V. N. Kushnir, S. L. Prischepa, J. Aarts, C. Bell, C. Cirillo, and C. Attanasio, The European Physical Journal B **80**, 445 (2011).

[18] A. K. Feofanov, V. A. Oboznov, V. V. Bol'ginov, J. Lisenfeld, S. Poletto, V. V. Ryazanov, A. N. Rossolenko, M. Khabipov, D. Balashov, A. B. Zorin, P. N. Dmitriev, V. P. Koshelets, and A. V. Ustinov, Nature Physics **6**, 593 (2010).

[19] L. Mattheiss, Physical Review B **1**, 373 (1970).

[20] J. De Vries, Thin Solid Films **167**, 25 (1988).

[21] A. R. Jani, N. E. Brener, and J. Callaway, Physical Review B **38**, 9425 (1988).

[22] J. H. Claassen, M. E. Reeves, and R. J. Soulen, Review of Scientific Instruments **62**, 996 (1991).

[23] S. J. Turneaure, E. R. Ulm, and T. R. Lemberger, Journal of Applied Physics **79**, 4221 (1996).

[24] S. J. Turneaure, A. A. Pesetski, and T. R. Lemberger, Journal of Applied Physics **83**, 4334 (1998).

[25] A. Kamlapure, M. Mondal, M. Chand, A. Mishra, J. Jesudasan, V. Bagwe, L. Benfatto, V. Tripathi, and P. Raychaudhuri, Applied Physics Letters **96** (2010).

[26] T. R. Lemberger, I. Hetel, J. W. Knepper, and F. Y. Yang, Physical Review B - Condensed Matter and Materials Physics **76**, 094515 (2007).

[27] M. Houzet and J. S. Meyer, Physical Review B **80**, 012505 (2009).

[28] L. Tagirov, Physica C: Superconductivity **307**, 145 (1998).

[29] B. Predel, in *Phase Equilibria, Crystallographic and Thermodynamic Data of Binary Alloys: Ni-Np Pt-Zr*, edited by O. Madelung (Springer Berlin Heidelberg, 1998) pp. 1–3.